

Multivariate optimization and kinetics for treatment of fracturing flowback fluids with *Chlorella vulgaris*

Ran Li^{a,b,c}, Jie Pan^a, Li Zhang^d, Yang Liu^{a,c,*}

^aCollege of Petroleum Engineering, Xi'an Shiyou University, Xi'an 710065, Shaanxi Province, China, Tel. +1 780 492 0249; Fax: +1 780 492 5115; emails: yang.liu@ualberta.ca (Y. Liu), rli@xsyu.edu.cn (R. Li), jackpan@xsyu.edu.cn (J. Pan)

^bTechnology Center of High Energy Gas Fracturing, CNPC, Xi'an Shiyou University, Xi'an 710065, Shaanxi Province, China

^cDepartment of Civil and Environmental Engineering, University of Alberta, Edmonton, Alberta, T6G 1H9, Canada

^dPetroleum Engineering Institute of Zhongyuan Petroleum oilfield, Puyang 457000, Henan Province, China, email: 645899357@qq.com (Li. Zhang)

Received 9 August 2019; Accepted 13 January 2020

ABSTRACT

Fracturing flowback fluids were biologically treated with *Chlorella vulgaris*. Individual and interactive effects of three variables – the dilution ratio of fracturing flowback fluids, the β -mannanase dose, and the powder activated carbon (PAC) dose – on chemical oxygen demand (COD) removal efficiency and algal density were optimized by response surface methodology combined with a Box–Behnken design. Treatment efficiency and algal density were affected most by the dilution ratio. Optimal conditions for algal growth and proliferation comprised a dilution ratio of 1:3, no β -mannanase, a PAC dose of 50 mg/L, and a maximum algal density was 2.51 g/L. The experimental data agreed well with the model-predicted COD removal efficiency (42.61% vs. 45.27%) under the optimum conditions of a dilution ratio of 1:5, a β -mannanase dose of 135.28 mg/L, and a PAC dose of 50 mg/L. A kinetic equation representing organic compound biodegradation by *C. vulgaris* was established, and the degradation half-life of COD was 132.63 h.

Keywords: *Chlorella vulgaris*; Fracturing flowback fluids; Biodegradation; Box–Behnken design

1. Introduction

Hydraulic fracturing is widely used to enhance the productivity of low- and extra-low-permeability oil-gas wells. Approximately 60% of wells produce natural gas and petroleum with fracking, which has reduced the oil and gas prices in the past few years [1–4]. During the fracturing process, water containing chemical additives and a propping agent is injected into the oil-gas wells under high pressure to fracture the rock formation [1]. After about two weeks, 10%–30% of the fracking water returns to the surface as “flowback” and contains released oil or gas and other dissolved chemicals that can pollute the environment [5–8]. Research on

fracturing flowback fluids indicates that flow-back contains about 134 chemicals that are mostly nontoxic or low-toxicity substances [9,10], thus biological processing of flowback fluids is feasible [11–14]. However, new biological technologies are needed to reduce capital and system operating costs and minimize the environmental impacts of fracturing wastewater treatment.

Microalgal wastewater remediation has been widely studied in recent years, with most studies focused on animal and municipal wastewater treatment [15–17]. Microalgae biomass is a promising feedstock for biofuels, as it can achieve both organic matter removal and biodiesel production in wastewater treatment, leading to economic benefits

* Corresponding author.

[18,19]. Many factors are affecting the growth of microalgae such as mediums, additives, and culture conditions [20–23]. Response surface methodology (RSM), an efficient technique in evaluating the effect of parameters on treatment results, is a collection of mathematical and statistical techniques, which can be used to evaluate the relative significance of different affecting factors and estimate the interaction effects between the factors [24,25]. Nowadays, Box–Behnken design (BBD), an RSM design, is useful in developing, improving, and optimizing processes, considering its advantages such as requiring less design points [26]. However, there is little research on the algal treatment of fracturing flowback fluids with complex chemicals and high concentration. Impacts of influencing factors on the algal biomass production and organics removal rate in fracturing wastewater treatment with microalgae are also unclear.

In this study, fracturing flowback fluids were biologically treated with *Chlorella vulgaris*. β -mannanase was used to hydrolyze polysaccharide from fracturing flowback fluids into monosaccharides to provide a carbon source for heterotrophic growth of algae. Continuous variable surface equations comprising an RSM combined with a BBD were designed to investigate how three factors – dilution ratio of fracturing flowback fluids, β -mannanase dose, powder activated carbon (PAC) dose – would affect chemical oxygen demand (COD) removal efficiency and algal density in a *Chlorella*-treated fracturing flowback fluid. Quadratic multi-factor regression equations comprising the three factors and the desired responses were built via RSM-BBD and used to optimize the three factors and uncover the rules of two-factor interactions. A kinetic equation representing organic compound biodegradation by algae in wastewater was established.

2. Materials and methods

2.1. Materials

C. vulgaris was purchased from the Institute of Hydrobiology, Chinese Academy of Sciences. Fracturing flowback fluid was prepared as follows: 3.5 g/L hydroxypropyl guar gum, 1.2 g/L Na_2CO_3 , and 40 g/L KCl were added to tap water and stirred to form a base fluid. The base fluid was mixed with 24 g/L sodium tetraborate and aged for 12 h to form a fracturing fluid. Ammonium persulfate (0.2 g/L) was then added to the fracturing fluid and the solution was heated at 80°C for 1 h.

2.2. Preparation of immobilized *C. vulgaris* beads

C. vulgaris cells were cultivated in a 1 L bottle containing 0.6 L of the BG11 medium [27]. Algal cells were harvested in the exponential growth phase (1 d after inoculation), concentrated by centrifugation at 4,000 r/min for 10 min using a centrifuge (Xinkang Co., China), and re-suspended in 50 mL of distilled water to form an algal suspension. The algal suspension was mixed with 3% sodium alginate and PAC (particle size of 74 μm) to form an algal-alginate-PAC suspension, which was titrated into a 3% CaCl_2 solution at 1 mL/min to produce 4 mm-diameter algal beads. The algal beads were allowed to crosslink for 10 h, then washed and soaked with distilled water.

2.3. Bath cultures

Algal beads (150 beads) were cultivated for 7 d at 25°C in 100 mL of fracturing flowback fluid at an illumination intensity of 4,000 lux using light/dark alternations of 16 h/8 h. Algal beads and flowback fluids were then separated, and the COD was quantified using the COD measurement system and kit (Lianhua Technology, China). Algal gel balls were then added to a 1.5% sodium citrate solution to form an algal suspension, which was detected at 658 nm on the spectrophotometer; an alga-free medium was used as a blank control. The algal cell density (DW) in the culture medium was determined according to Eq. (1):

$$DW = 0.4818 \times OD_{658}, R^2 = 0.9932 \quad (1)$$

where DW is in g/L, and OD_{658} is the difference in optical density at 658 nm between the algae-containing water sample and the algae-free medium.

2.4. Response surface methodology-Box–Behnken design

Factors that were expected to influence the COD removal rate and algal density were optimized using RSM-BBD. The three process variables were the dilution ratio of fracturing flowback fluids, the dose of β -mannanase, and the dose of PAC, with the response being the COD removal rate or the algal density. Codes and levels of the independent variables are given in Table 1. After the selection of process variables and their ranges, experiments were established based on the BBD. The complete design consisted of 17 runs; the test data is shown in Table 2.

Experimental data were analyzed by the response surface regression procedure. The second-order polynomial was fitted via manual regression as follows:

$$Y = \beta_0 + \sum_{i=1}^n \beta_i X_i + \sum_{i=1}^n \beta_{ii} X_i^2 + \sum_{i=1}^n \sum_{j=1}^n \beta_{ij} X_i X_j + e \quad (2)$$

where Y is a response; β_0 is a constant; β_i ($i = 1, 2, 3$) is the linear effect of X_i ; β_{ij} is the interaction between X_i and X_j ; β_{ii} is the quadratic effect of X_i ; and X_i and X_j are the coded values of the independent variables [28]. Analysis of variance (ANOVA) and response surface trials were performed using Design Expert 10.0.

3. Results and discussion

3.1. Model build-up and ANOVA

According to the RSM-BBD results, linear and second-order polynomials were fitted to the experimental data

Table 1
Process variables, their codes, and their limits

Variable	Unit	Code	–1 level	0 level	+1 level
Dilution ratio	–	X_1	0	1:2.5	1:5
β -mannanase	mg/L	X_2	0	100	200
PAC	mg/L	X_3	0	25	50

Table 2
BBD matrix with three independent variables (coded values) and corresponding experimental and predicted algal densities

Std. run order	Coded value			COD removal rate (%)			Algal density (g/L)		
	X ₁	X ₂	X ₃	Expt. ^a	Pred. ^b	ε	Expt. ^a	Pred. ^b	ε
1	-1	-1	0	-8.09	-6.93	-1.16	0.32	0.53	-0.21
2	1	-1	0	23.66	27.35	-3.69	1.8	1.85	-0.05
3	-1	1	0	0.73	-2.96	3.69	0.34	0.29	0.05
4	1	1	0	37.40	36.24	1.16	1.91	1.70	0.21
5	-1	0	-1	4.61	8.03	-3.42	0.31	0.05	0.26
6	1	0	-1	32.45	33.33	-0.88	1.65	1.56	0.09
7	-1	0	1	-2.97	-3.85	0.88	0.34	0.43	-0.09
8	1	0	1	47.76	44.34	3.42	1.39	1.65	-0.26
9	0	-1	-1	24	19.42	4.58	1.68	1.73	-0.05
10	0	1	-1	24	24.27	-0.27	1.63	1.94	-0.31
11	0	-1	1	17.68	17.41	0.27	2.68	2.37	0.31
12	0	1	1	20.84	25.42	-4.58	1.81	1.77	0.04
13	0	0	0	29.85	29.38	0.47	2.05	2.06	-0.01
14	0	0	0	32.65	29.38	3.27	2.01	2.06	-0.05
15	0	0	0	31.08	29.38	1.70	1.83	2.06	-0.23
16	0	0	0	32.03	29.38	2.65	2.03	2.06	-0.03
17	0	0	0	21.27	29.38	-8.11	2.36	2.06	0.30

^aExpt. means experimental
^bPred. means model prediction

(Table 2) to obtain regression equations for the COD removal rate and the algal density against the three process variables, which are given in Eqs. (3) and (4), respectively:

$$Y_1 = 29.38 + 18.37X_1 + 3.22X_2 - 0.22X_3 + 1.23X_1X_2 + 5.72X_1X_3 + 0.97X_2X_3 - 8.56X_1^2 - 7.39X_2^2 - 0.35X_3^2 \quad (3)$$

where Y₁ is the COD removal rate, X₁ is the dilution ratio of fracturing flowback fluids, X₂ is the β-mannanase dose, and X₃ is the PAC dose.

$$Y_2 = 2.06 + 0.68X_1 - 0.10X_2 + 0.12X_3 + 0.02X_1X_2 - 0.72X_1X_3 - 0.21X_2X_3 - 1.00X_1^2 + 0.03X_2^2 - 0.14X_3^2 \quad (4)$$

where Y₂ is the algal density, X₁ is the dilution ratio of fracturing flowback fluids, X₂ is the β-mannanase dose, and X₃ is the PAC dose.

The ANOVA for the two quadratic response surface models are shown in Tables 3 and 4, respectively. Table 3 indicates that the second-order polynomial model, Eq. (3), is significant (*p* < 0.01) with R² = 0.9501, adjusted R² = 0.8860, and predicted R² = 0.5419. Table 4 shows that the second-order polynomial model, Eq. (4) is also significant, with a very small *p*-value (0.0022) and a satisfactory coefficient of determination (R² = 0.9348, Adj. R² = 0.8509, Pred. R² = 0.1908). X₁ is significant in the two models (*p* < 0.01) and lack-of-fit in both models is insignificant. It is evident that the dilution ratio of fracturing flowback fluids exerted the largest effect on the COD removal rate and the algal density.

As shown in Fig. 1, the predicted values and experimental values fit well for both the COD removal rate and the algal density, indicating the model developed here was

successful in capturing the correlation between influence factors and response factors. Furthermore, the absolute average deviation between predicted and observed data is very small in both cases – 2.6 in Eq. (3), 0.15 in Eq. (4). Thus, ANOVA and reliability analysis indicates that the model equations describe the experimental results adequately.

3.2. Effects of process variables

ANOVA indicates that relationships between the dilution ratio of fracturing flowback fluids, the β-mannanase dose, the PAC dose, and the COD removal rate of algal density are quadratic rather than linear. Three-dimensional response surfaces were simulated from Eqs. (3) and (4) to examine interactions between independent variables and responses (Figs. 2–4). These graphs represent the effects of two variables at their studied ranges with the third one maintained at zero level.

Fig. 2 shows the 3D response surfaces for the COD removal rate and algal density as a function of the fracturing flowback fluid dilution ratio and the β-mannanase dose at a constant PAC dose (25 mg/L). The COD removal efficiency increased with an increasing dilution ratio and an increasing β-mannanase dose and changed slightly when the β-mannanase dose > 150 mg/L. The algal density first increased and then decreased with an increasing dilution ratio. However, the algal density was not largely affected by the β-mannanase dose within the respective experimental range. *Chlorella*, a mixotrophic microalgae, can simultaneously use inorganic carbon through photosynthesis and use organic carbon via heterotrophy. When the dilution ratio increased, the concentrations of toxic and harmful substances decreased, thus

Table 3
ANOVA for COD removal rate

Source	Sum of squares	df	Mean square	F value	P value	Remarks ^a
Model	3,498.02	9	388.67	14.82	0.0009	Significant
X ₁	2,700.76	1	2,700.76	103.00	0.0000	Significant
X ₂	82.69	1	82.69	3.15	0.1190	
X ₃	0.38	1	0.38	0.01	0.9072	
X ₁ X ₂	6.05	1	6.05	0.23	0.6456	
X ₁ X ₃	130.99	1	130.99	5.00	0.0605	
X ₂ X ₃	2.50	1	2.50	0.10	0.7666	
X ₁ ²	308.47	1	308.47	11.76	0.0110	Significant
X ₂ ²	230.05	1	230.05	8.77	0.0210	Significant
X ₃ ²	0.53	1	0.53	0.02	0.8911	
Error	183.54	7	26.22			
Lack of fit	96.95	3	32.32	1.49	0.3445	Not significant
Pure error	86.60	4	21.65			
Total	3,681.56	16				

^aR² = 0.9501, Adj. R² = 0.8860, Pred. R² = 0.5419

Table 4
ANOVA for algal density

Source	Sum of squares	df	Mean square	F value	P value	Remarks ^a
Model	8.41	9	0.93	11.14	0.0022	Significant
X ₁	3.70	1	3.70	44.11	0.0003	Significant
X ₂	0.08	1	0.08	0.93	0.3670	
X ₃	0.11	1	0.11	1.35	0.2842	
X ₁ X ₂	0.00	1	0.00	0.02	0.8809	
X ₁ X ₃	0.02	1	0.02	0.25	0.6320	
X ₂ X ₃	0.17	1	0.17	2.00	0.1998	
X ₁ ²	4.17	1	4.17	49.75	0.0002	Significant
X ₂ ²	0.00	1	0.00	0.05	0.8271	
X ₃ ²	0.08	1	0.08	0.96	0.3608	
Error	0.59	7	0.08			
Lack of fit	0.44	3	0.15	4.02	0.1063	Not Significant
Pure error	0.15	4	0.04			
Total	9.00	16				

^aR² = 0.9348, Adj. R² = 0.8509, Pred. R² = 0.1908

both algal density and COD removal efficiency increased. When the dilution ratio was too high, there was not enough carbon for the heterotrophic growth of *C. vulgaris*, so the algal density decreased. The β -mannanase influence on the COD removal rate and algal density can be explained by the fact that some of the *Chlorella* cells leaked out of the algal beads. In this study, a guar-based compound was used as the thickener of fracturing fluids. Guar gum consists of a β -(1,4)-linked D-mannan backbone with branch points of α -D-galactose units attached by (1 \rightarrow 6) linkages [29]. When the β -mannanase dose increased, β -mannanase broke guar gum into monosaccharides and thereby promoted *Chlorella* cells inside or outside the algal beads to degrade and accumulate organic pollutants, which is consistent

with previous research [30,31]. Thus, the COD removal rate increased, but the density of algal beads did not increase by much. When the β -mannanase dose was increased to some extent, most guar gum was broken down, so the COD removal rate did not increase further.

The effects of the fracturing flowback fluid dilution ratio and the PAC dose on COD-removal and algal density at a constant β -mannanase dose (100 mg/L) are shown in Fig. 3. Clearly, both the COD removal efficiency and the algal density first increased and then decreased with an increasing dilution ratio. PAC barely affected the COD removal rate and slightly increased the algal density. A previous study showed that activated carbon could mitigate the microalgal lysis caused by bacteria and thus increased the dry weight

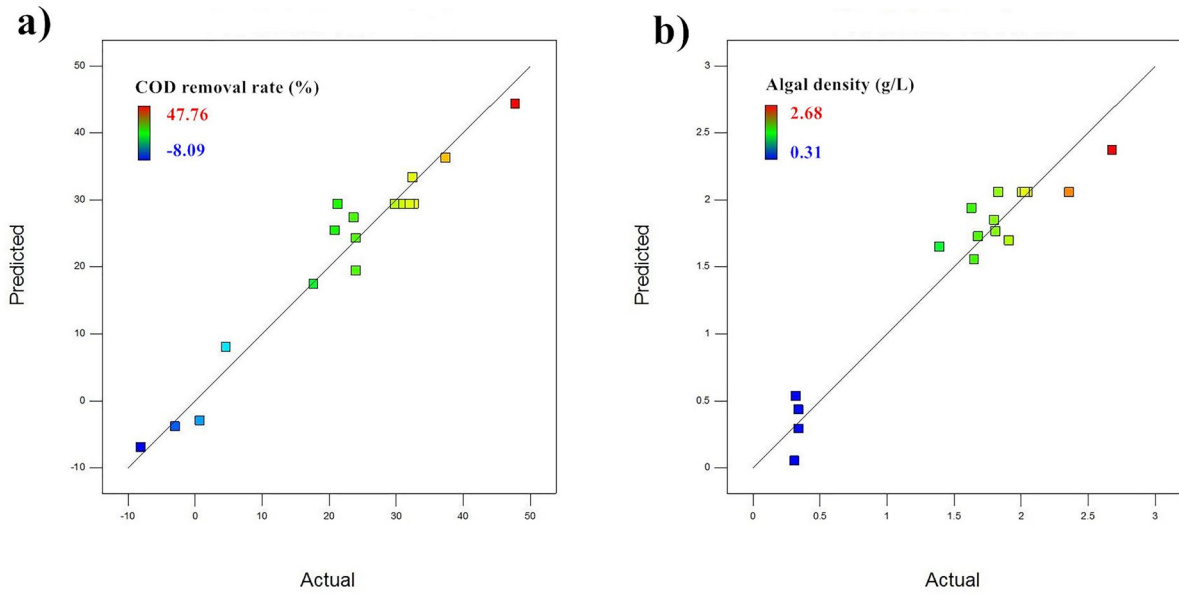


Fig. 1. Fitness of predictive value and experimental value of (a) COD removal rate and (b) algal density.

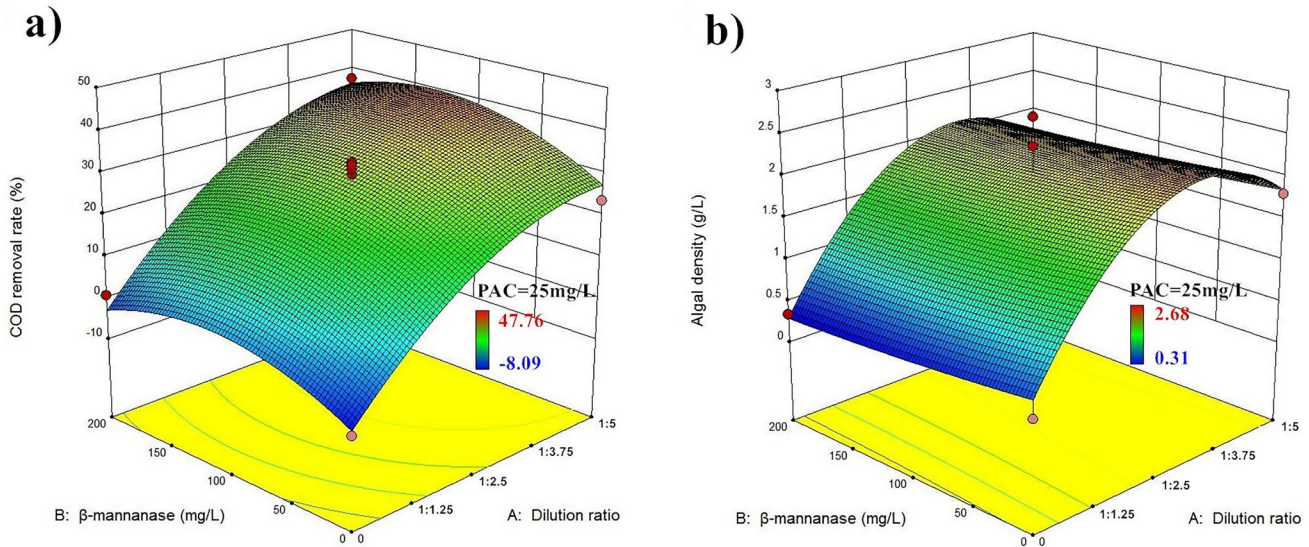


Fig. 2. 3D surface graph of the effects of the dilution ratio and β -mannanase dose on the (a) COD removal rate and (b) the algal density.

of microalgae [32], which is in agreement with the results observed in the present study.

The surface sizes of the graphs in Fig. 4 represent the combined effect of β -mannanase and PAC at constant dilution ratios of 1:2.5, suggesting that the COD removal efficiency first increased and then stabilized with increasing β -mannanase. The PAC dose barely affected the COD removal rate. The algal density increased as PAC increased, but changed only a little as β -mannanase increased.

3.3. Optimum condition and verification

The point prediction option in Design Expert 10.0 was used to accurately optimize variables. Experiments were

conducted under optimal operational conditions to verify the effects of the dilution ratio of fracturing flowback fluids, the β -mannanase dose, and the effects of PAC dose on COD removal efficiency and algal density. Optimized variables obtained from the statistical software and experimental values are listed in Table 5. The *C. vulgaris* bead treatment of fracturing flowback fluids under optimal conditions is illustrated in Fig. 5. Clearly, the *C. vulgaris* in the beads grew well, and the flowback fluids treated with *C. vulgaris* were clear. Table 5 summarizes the predicted responses in each setting of variables and the confirmation values obtained from the experiments. The optimal conditions were validated by two experiments using different optimized parameters and the errors of COD removal efficiency (response 1)

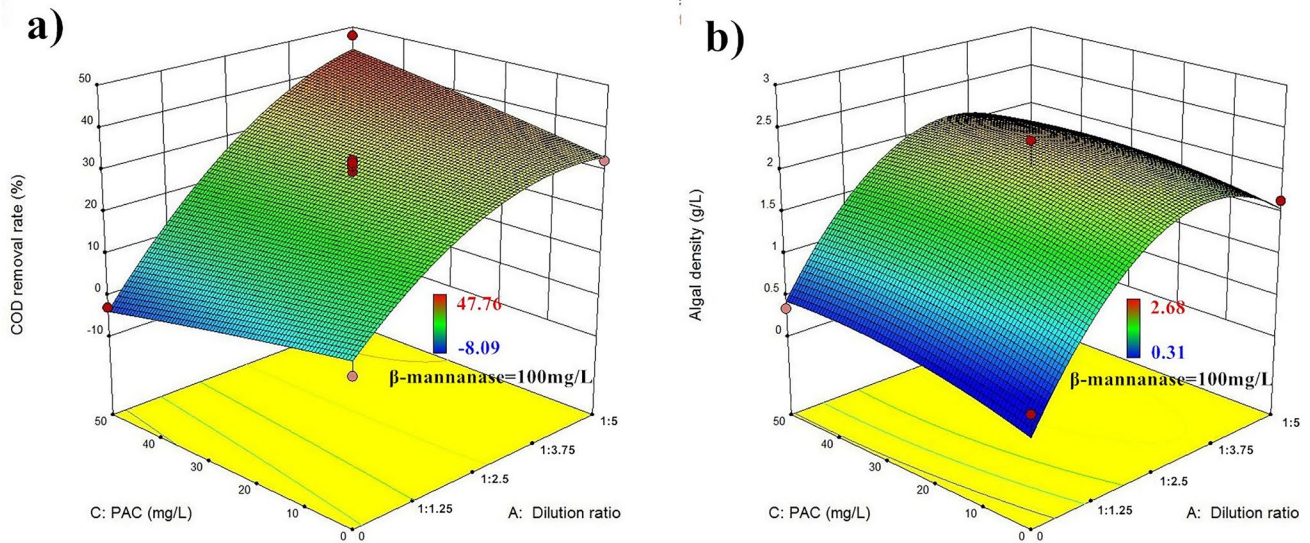


Fig. 3. 3D surface graph showing the effects of the dilution ratio and the PAC dose on the (a) COD removal rate and (b) the algal density.

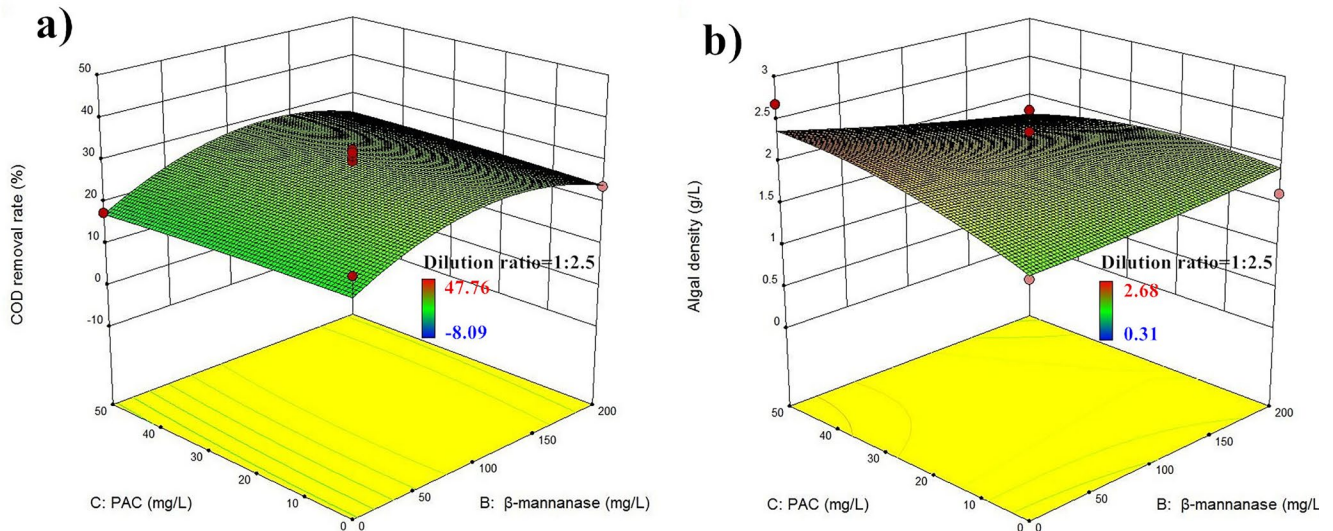


Fig. 4. 3D surface graph showing the (a) COD removal rate and (b) the algal density in the presence of increasing β -mannanase and increasing PAC.

and algal density (response 2) were determined to be 2.66% and 0.05 g/L, respectively. The agreement between predicted and experimental results verified the model's validity and the existence of an optimal point. This finding indicates that RSM-BBD is a reliable tool for determining the optimal values of individual factors.

3.4. Establishment of a kinetic equation

Algal cell density and biodegradative activity at different growth stages have been reported to affect the algal biodegradation rate of organic compounds [33]. Based on the Monod first-order kinetic equation ($-dC/dt = KN$), the kinetic Eq. (5) of organic compound biodegradation by algae is:

$$-\frac{dC}{dt} = K_1NU \tag{5}$$

where C is the concentration of organic compound (mg/L), t is time (h), K_1 is a constant, N is the algal density (g/L), and U is the biodegradative activity of the algae.

If U is linearly related to the algal growth rate (dN/dt),

$$-\frac{dC}{dt} = KN \frac{dN}{dt}, \int dC = -K \int N dN, \text{ and } C = -\frac{1}{2}KN^2 + C_0 \tag{6}$$

where C_0 is a constant.

Algal density can be expressed as [34]:

Table 5
Optimum and confirmative values of the process variables for maximum responses

Dilution ratio	β -mannanase (mg/L)	PAC (mg/L)		Response	
				Optimized values (Predicted values)	Confirmation values (Actual values)
1:5	135.28	50.00	COD removal rate (%)	45.27	42.61
1:3	0.00	50.00	Algal density (g/L)	2.46	2.51

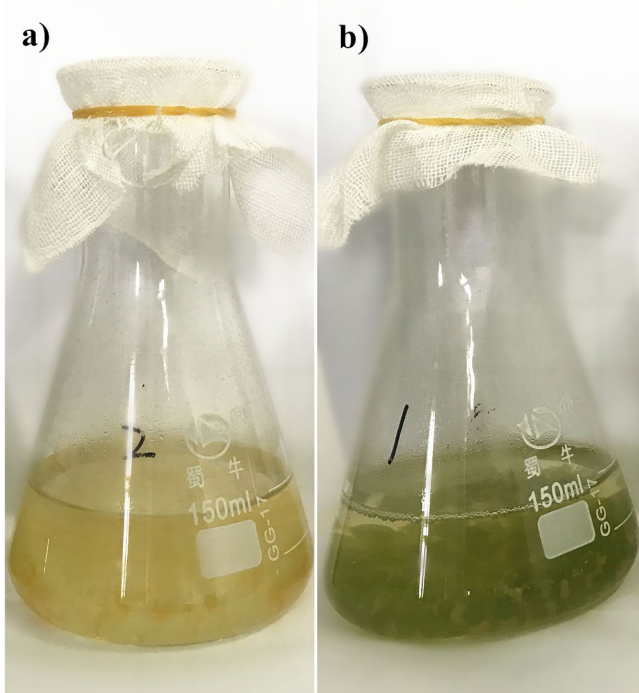


Fig. 5. (a) Before and (b) after fracturing flowback fluid is treated with *Chlorella vulgaris*.

$$N = \frac{N_c}{1 + \left(\frac{N_c}{N_0} - 1\right) e^{-g(t-t_0)}} \quad (7)$$

where N_c is the carrying capacity, g is the biotic potential, N_0 is the initial algal density, and t_0 is the initial time.

At time intervals t_1 , t_2 , and t_3 and corresponding algal densities N_1 , N_2 , and N_3 [35],

$$N_c = \frac{N_2(2N_1N_3 - N_1N_2 - N_2N_3)}{N_1N_3 - N_2^2} \quad \text{and} \quad (8)$$

$$g = -\frac{\ln \frac{N_c - N_e}{N_e} - \ln \frac{N_c - N_0}{N_0}}{t - t_0} \quad (9)$$

where N_e is the algal density at the end of the treatment.

In the biotreatment, the observed *C. vulgaris* densities at 0, 60, 84, and 108 h were 0.17, 0.31, 0.51, and 0.62 g/L,

respectively. The N_c and g calculated from Eqs. (8) and (9) were 0.68 g/L and 0.03, respectively. The second-order constant K and the constant C_0 can be determined by a linear regression of Eq. (6) between observed COD concentrations and the square of algal densities observed at different periods. The change in the organic compound concentration C in fracturing wastewater treated with *C. vulgaris* over time is represented by:

$$C = -5415.88 \left(\frac{0.68}{1 + 3e^{-0.03t}} \right)^2 + 4893.23 \quad R^2 = 0.8130 \quad (10)$$

The degradation half-life of an organic pollutant determined in Eq. (10) was 132.63 h, indicating an efficient treatment of fracturing wastewater by *C. vulgaris*.

4. Conclusions

In this study, the technical feasibility of coupling fracturing wastewater treatment with algal biomass production was evaluated. The RSM and the BBD were successfully combined to analyze linear, quadratic, and interactive effects of fracturing flowback fluid dilution ratio, β -mannanase dose, and PAC dose on the COD removal rate and the algal density in fracturing flowback fluids biologically treated with *C. vulgaris*. Under optimized process conditions (dilution ratio of 1:5, β -mannanase dose of 135.28 mg/L, PAC dose of 50 mg/L), the COD removal rate was 42.61%. The optimum condition for maximum algal density was a dilution ratio of 1:3 with no β -mannanase and a PAC dose of 50 mg/L; the algal density was 2.51 g/L. A kinetic equation for organic compound biodegradation by algae indicated a degradation half-life of COD of 132.63 h.

Acknowledgements

This study was supported by the National Natural Science Foundation of China (No. 51504192, No. 51904245), the Natural Science Basic Research Plan of Shaanxi Province (No.2016JQ5102), the Scientific Research Program funded by the Shaanxi Provincial Education Department (No.17JK0616), and The Youth Talent Collection Program of Universities in Shaanxi (No.20160119).

References

[1] T.J. Gallegos, B.A. Varela, S.S. Haines, M.A. Engle, Hydraulic fracturing water use variability in the United States and potential environmental implications, *Water Resour. Res.*, 51 (2015) 5839–5845.

- [2] D.J. Miller, X. Huang, H. Li, S. Kasemset, A. Lee, D. Agnihotri, T. Hayes, D.R. Paul, B.D. Freeman, Fouling-resistant membranes for the treatment of flowback water from hydraulic shale fracturing: a pilot study, *J. Membr. Sci.*, 437 (2013) 265–275.
- [3] C.T. Montgomery, M.B. Smith, Hydraulic fracturing: history of an enduring technology, *J. Pet. Technol.*, 62 (2010) 26–40.
- [4] S. Rassenfoss, From flowback to fracturing: water recycling grows in the Marcellus Shale, *J. Pet. Technol.*, 63 (2011) 48–51.
- [5] M.C. Brittingham, K.O. Maloney, A.M. Farag, D.D. Harper, Z.H. Bowen, Ecological risks of shale oil and gas development to wildlife, aquatic resources and their habitats, *Environ. Sci. Technol.*, 48 (2014) 11034–11047.
- [6] A.J. Kondash, E. Albright, A. Vengosh, Quantity of flowback and produced waters from unconventional oil and gas exploration, *Sci. Total Environ.*, 574 (2017) 314–321.
- [7] A. Altaee, N. Hilal, Dual-stage forward osmosis/pressure retarded osmosis process for hypersaline solutions and fracking wastewater treatment, *Desalination*, 350 (2014) 79–85.
- [8] J.P. Nicot, B.R. Scanlon, R.C. Reedy, R.A. Costley, Source and fate of hydraulic fracturing water in the Barnett Shale: a historical perspective, *Environ. Sci. Technol.*, 48 (2014) 2464–2471.
- [9] J.M. Estrada, B. Rao, A review of the issues and treatment options for wastewater from shale gas extraction by hydraulic fracturing, *Fuel*, 182 (2016) 292–303.
- [10] E.E. Yost, J. Stanek, R.S. Dewoskin, L.D. Burgoon, Overview of chronic oral toxicity values for chemicals present in hydraulic fracturing fluids, flowback, and produced waters, *Environ. Sci. Technol.*, 50 (2016) 4788–4797.
- [11] G.A. Lutz, N.T. Dunford, Algal treatment of wastewater generated during oil and gas production using hydraulic fracturing technology, *Environ. Technol.*, 40 (2019) 1027–1034.
- [12] N.R. Mullins, A.J. Daugulis, The biological treatment of synthetic fracking fluid in an extractive membrane bioreactor: selective transport and biodegradation of hydrophobic and hydrophilic contaminants, *J. Hazard. Mater.*, 371 (2019) 734–742.
- [13] B. Akyon, D. Lipus, K. Bibby, Glutaraldehyde inhibits biological treatment of organic additives in hydraulic fracturing produced water, *Sci. Total Environ.*, 666 (2019) 1161–1168.
- [14] A. Butkovskyi, A.H. Faber, Y. Wang, K. Grolle, R. Hofman-Caris, H. Bruning, A.P. Van Wezel, H.H. Rijnaarts, Removal of organic compounds from shale gas flowback water, *Water Res.*, 138 (2018) 47–55.
- [15] D. García, E. Posadas, S. Blanco, G. Acién, P. García-Encina, S. Bolado, R. Muñoz, Evaluation of the dynamics of microalgae population structure and process performance during piggery wastewater treatment in algal-bacterial photobioreactors, *Bioresour. Technol.*, 248 (2018) 120–126.
- [16] Q. Wang, W. Jin, X. Zhou, S. Guo, S.H. Gao, C. Chen, R. Tu, S.F. Han, J. Jiang, X. Feng, Growth enhancement of biodiesel-promising microalga *Chlorella pyrenoidosa* in municipal wastewater by polyphosphate-accumulating organisms, *J. Cleaner Prod.*, 240 (2019) 118148.
- [17] P. Folori, S. Petrini, G. Andreottola, Evolution of real municipal wastewater treatment in photobioreactors and microalgae-bacteria consortia using real-time parameters, *Chem. Eng. J.*, 345 (2018) 507–516.
- [18] R.H. Wijffels, M.J. Barbosa, An outlook on microalgal biofuels, *Science*, 329 (2010) 796–799.
- [19] R. Li, J. Yang, J. Pan, L. Zhang, W. Qin, Effect of immobilization on growth and organics removal of *Chlorella* in fracturing flowback fluids treatment, *J. Environ. Manage.*, 226 (2018) 163–168.
- [20] A.M. Hamed, S.K. Prajapati, S. Simsek, H. Simsek, Growth regime and environmental remediation of microalgae, *Algae*, 31 (2016) 189–204.
- [21] L. Liu, Y. Zhao, X. Jiang, X. Wang, W. Liang, Lipid accumulation of *Chlorella pyrenoidosa* under mixotrophic cultivation using acetate and ammonium, *Bioresour. Technol.*, 262 (2018) 342–346.
- [22] J.I. Labbé, J.L. Ramos-Suárez, A. Hernández-Pérez, A. Baeza, F. Hansen, Microalgae growth in polluted effluents from the dairy industry for biomass production and phytoremediation, *J. Environ. Chem. Eng.*, 5 (2017) 635–643.
- [23] Z.Y. Liu, G.C. Wang, B.C. Zhou, Effect of iron on growth and lipid accumulation in *Chlorella vulgaris*, *Bioresour. Technol.*, 99 (2008) 4717–4722.
- [24] S.C. Ferreira, R.E. Bruns, H.S. Ferreira, G.D. Matos, J.M. David, G.C. Brandao, E.G.P. Da Silva, L.A. Portugal, P.S. Dos Reis, A.S. Souza, W.N.L. Dos Santos, Box–Behnken design: an alternative for the optimization of analytical methods, *Anal. Chim. Acta*, 597 (2007) 179–186.
- [25] M. Mourabet, A. El Rhilassi, H. El Boujaady, M. Bennani-Ziatni, R. El Hamri, A. Taitai, Removal of fluoride from aqueous solution by adsorption on *Apatitic tricalcium phosphate* using Box–Behnken design and desirability function, *Appl. Surf. Sci.*, 258 (2012) 4402–4410.
- [26] R. Ragonese, M. Macka, J. Hughes, P. Petocz, The use of the Box–Behnken experimental design in the optimization and robustness testing of a capillary electrophoresis method for the analysis of ethambutol hydrochloride in a pharmaceutical formulation, *J. Pharm. Biomed. Anal.*, 27 (2002) 995–1007.
- [27] P. Singh, A. Guldhe, S. Kumari, I. Rawat, F. Bux, Investigation of combined effect of nitrogen, phosphorus and iron on lipid productivity of microalgae *Ankistrodesmus falcatus*, kj671624 using response surface methodology, *Biochem. Eng. J.*, 94 (2015) 22–29.
- [28] J.F. Fu, Y.Q. Zhao, X.D. Xue, W.C. Li, A.O. Babatunde, Multivariate-parameter optimization of acid blue-7 wastewater treatment by Ti/TiO₂ photoelectrocatalysis via the Box–Behnken design, *Desalination*, 243 (2009) 42–51.
- [29] N. Thombare, U. Jha, S. Mishra, M.Z. Siddiqui, Guar gum as a promising starting material for diverse applications: a review, *Int. J. Biol. Macromol.*, 88 (2016) 361–372.
- [30] Y.X. Li, P. Yi, N.N. Wang, J. Liu, X.Q. Liu, Q.J. Yan, Z.Q. Jiang, High-level expression of β -mannanase (RmMan5A) in *Pichia pastoris* for partially hydrolyzed guar gum production, *Int. J. Biol. Macromol.*, 105 (2017) 1171–1179.
- [31] B. Jiang, Z. Sun, Y. Hou, L. Yang, F. Yang, X. Chen, X. Li, Isolation and properties of an endo- β -mannanase-producing *Bacillus* sp. lx114 capable of degrading guar gum, *Prep. Biochem. Biotechnol.*, 46 (2015) 495–500.
- [32] Z.Y. Ni, J.Y. Li, Z.Z. Xiong, L.H. Cheng, X.H. Xu, Role of granular activated carbon in the microalgal cultivation from bacteria contamination, *Bioresour. Technol.*, 247 (2018) 36–43.
- [33] H. Yan, C. Ye, C. Yin, Kinetics of phthalate ester biodegradation by *Chlorella pyrenoidosa*, *Environ. Toxicol. Chem.*, 14 (1995) 931–938.
- [34] B. Richard, Principles of Ecology, Saunders College Publisher, Philadelphia, PA, 1988.
- [35] K. Xu, Biological Mathematics, Chinese Academy of Sciences, Beijing, China, 1988.